

Thermomagnonic diode: Rectification of energy and magnetization currentsSimone Borlenghi,^{1,*} Stefano Lepri,^{2,3} Lars Bergqvist,^{1,4} and Anna Delin^{1,4,5}¹*Department of Materials and Nanophysics, School of Information and Communication Technology, Electrum 229, Royal Institute of Technology, SE-16440 Kista, Sweden*²*Consiglio Nazionale delle Ricerche, Istituto dei Sistemi Complessi, Via Madonna del Piano 10, I-50019 Sesto Fiorentino, Italy*³*Istituto Nazionale di Fisica Nucleare, Sezione di Firenze, via G. Sansone 1, I-50019 Sesto Fiorentino, Italy*⁴*SeRC (Swedish e-Science Research Center), KTH, SE-10044 Stockholm, Sweden*⁵*Department of Physics and Astronomy, Uppsala University, Box 516, SE-75120 Uppsala, Sweden*

(Received 1 November 2013; revised manuscript received 3 February 2014; published 26 February 2014)

We investigate the dynamics of two coupled macrospins connected to thermal baths at different temperatures. The system behaves like a diode which allows the propagation of energy and magnetization currents in one direction only. This effect is described by a simple model of two coupled nonlinear oscillators interacting with two independent reservoirs. It is shown that the rectification phenomenon can be interpreted as a stochastic phase synchronization of the two spin oscillators. A brief comparison with realistic micromagnetic simulations is presented. This new effect yields promising opportunities in spin caloritronics and nanophononic devices.

DOI: [10.1103/PhysRevB.89.054428](https://doi.org/10.1103/PhysRevB.89.054428)

PACS number(s): 75.76.+j, 05.10.Gg, 75.78.Cd

I. INTRODUCTION

Since the discovery of the spin-Seebeck effect [1,2], according to which a thermal gradient in a ferromagnet generates a spin current, the emerging field of spin caloritronics [3] has been the object of intense investigation. A related line of research, which was developed independently in recent years, focuses on heat transport in lattices of nonlinear oscillators [4,5]. The relevance of such studies to condensed-matter problems is illustrated by the growing interest in heat transport properties of low-dimensional materials like nanotubes [6] and graphene [7]. Further motivation comes from the perspective of controlling nanoscale energy flows [8,9] as well as from the hope of finding novel dynamical mechanisms that could enhance the efficiency of thermoelectric energy conversion [10].

Within this general background, in the present work, we investigate theoretically a system that could be the building block of novel magnonic devices, allowing the propagation of energy and magnetization currents in one direction only. The system consists of two coupled macrospins connected to thermal reservoirs at different temperatures. It has been demonstrated recently by means of micromagnetic simulations that such a system can indeed act a spin-Seebeck diode [11]. The basic functioning principle is similar to that of the thermal diode considered in the recently born field of phononics [7–9,12,13]. It can be qualitatively explained in terms of a temperature-dependent renormalization of the macrospin frequency spectra, whose overlap may lead to a conducting or nonconducting state depending on the sign of the applied thermal gradient. However, such a thermomagnonic system offers several new possibilities for control of nanoscale energy flows [14]. The most evident one is related to the fact that we are dealing here with *two coupled currents* of the basic conserved quantities, energy and magnetization.

To gain theoretical insight we study here an effective simplified model consisting of two coupled oscillators interacting

with external reservoirs. This will allow us to place on a clearer basis the basic operating principles of the system. In particular, we argue that the rectification effect can be described as *stochastic phase synchronization* [15–18] of the two precessing spins. Stochastic phase synchronization occurs in a large class of nonlinear oscillators driven by noise. It basically amounts to the fact that noise can lead to an enhanced phase entrainment and thus to an increase in energy transfer among the oscillators. This phenomenon, which has attracted great interest in the past decade in connection with biomedical systems and neural circuits [19,20], has never been investigated in the broad context of nanoscale energy transfer or, in particular, in magnonics and spin caloritronics. Such a novel interpretation, which is pursued in the present work, is useful to ease the physical intuition and to suggest a new mechanism for the transfer of energy and spin currents in these systems.

The present study answers a very general question, that is, under what conditions the transfer of energy and magnetization between coupled spins at different temperatures occurs. The rectification effect considered here has several applications. In particular, it opens the way to the experimental realization of thermal logic gates, which have been recently described theoretically within the field of nanophononics [21–23]. This could be the starting point of a new generation of energy-efficient electronic devices.

Moreover, we suggest implementing this new diode using a very common and well-known spintronics device, the spin valve. We wish to point out that the studies on the spin-Seebeck effect on spin-valve systems performed so far concern only the spin current carried by electrons. The notion of magnetization current developed here, which is a special case of the usual spin-wave (SW) current, has not been investigated so far in this kind of system. Spin-caloritronics experiments are challenging due to the intrinsic difficulty of measuring the spin current, which is based on the inverse spin-Hall effect [1]. Here, we suggest a *direct* way to detect spin and energy transport, which is based on the overlap of the SW modes of the system. This can be done using various well-known techniques, such as ferromagnetic resonance force spectroscopy [24,25].

*simonebg@kth.se

The paper is organized as follows. In Sec. II we describe the physical system and introduce the effective coupled-oscillator model and its interaction with the thermal reservoirs. In Sec. III we discuss the rectification of energy and magnetization currents as a phase-synchronization phenomenon induced by thermal fluctuations. Some simulations of the oscillator model are thereby described. In Sec. IV we consider the case in which the system is driven by both a thermal and a magnetization gradient. The predictions of the models are then tested qualitatively with the micromagnetic simulations of the full magnetization dynamics of the device (Sec. V). Finally, we close the paper with an overview in the concluding section.

II. PHYSICAL SYSTEM AND MODEL

The local dynamics of the magnetization \mathbf{M} in a ferromagnet is described by the Landau-Lifshitz-Gilbert (LLG) equation [26–28]

$$\frac{\partial \mathbf{M}}{\partial t} = -\gamma_0 \mathbf{M} \times \mathbf{H}_{\text{eff}} + \alpha \mathbf{M} \times \frac{\partial \mathbf{M}}{\partial t} / M_s, \quad (1)$$

where γ_0 is the gyromagnetic ratio, α is the adimensional Gilbert damping parameter, and \mathbf{H}_{eff} is the effective field, given by the functional derivative of the Gibbs free energy of the system with respect to the magnetization. In our case, the effective field contains the applied, exchange, and dipolar fields. The first term on the right-hand side of Eq. (1) describes the precession of the magnetization around the effective field with frequency $\omega = \gamma_0 |\mathbf{H}_{\text{eff}}|$, while the second term accounts for energy losses at a rate proportional to the Gilbert damping parameter α .

It is known that an electrical current with spin polarization \mathbf{p} exerts a spin transfer torque (STT) on the localized magnetic moments of a ferromagnet [29,30]. The effect of STT is described by rescaling the effective field as $\mathbf{H}_{\text{eff}} \rightarrow \mathbf{H}_{\text{eff}} - a\mathbf{p}$ and by adding to the right-hand side of Eq. (1) the term

$$\boldsymbol{\tau} = \gamma_0 \frac{b}{M_s} \mathbf{M} \times (\mathbf{M} \times \mathbf{p}). \quad (2)$$

The term proportional to a is usually called the fieldlike component of STT. The term proportional to b , which controls the damping, is the usual Slonczewski STT [31–35]. The latter can lead to a steady-state precession and to a reversal of the magnetization [36,37].

The parameters (a, b) are proportional to the intensity of the current and to the degree of spin polarization. In general, they both depend on the geometry of the system and on the microscopic transport properties of the material [38]. For their computation in realistic devices, several methods have been developed [39–42]. Here, they are considered free parameters of the model, which can be used to control the rectification effect.

The device considered here, shown in Fig. 1(a), consists of a spin-valve nanopillar made of two ferromagnetic layers separated by a nonmagnetic spacer and coupled by dipolar interaction. This system, which is the prototype for spintronic devices, has several applications [25,43] and constitutes the usual geometry for spin-transfer nano-oscillators (STNOs).

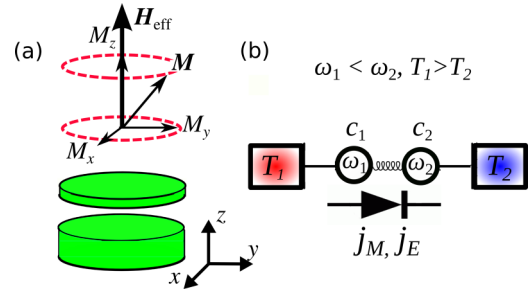


FIG. 1. (Color online) (a) Circular precession of the magnetization in a system of two disks coupled via dipolar interaction. (b) The system behaves as a chain of two oscillators with frequencies $\omega_1 < \omega_2$ connected to two thermal baths. Regarding the rectification effect, when $\Delta T = T_1 - T_2 > 0$ the two frequencies may overlap, giving the two nonzero currents j_M and j_E ; and when $\Delta T < 0$ the frequencies split, and no net current flows in the system.

We consider the simple case where both the effective field and the polarization vectors are aligned with the z axis, which defines the precession axis of the magnetization. In this case, the nonadiabatic STT leads simply to a rescaling of the oscillation frequency. Thus, in our model the relevant physics is described only by the Slonczewski STT. This simplification is quite realistic if we consider the nanopillar geometry [24,25,33].

Within the macrospin approximation, the circular precession in the x - y plane of the magnetization vectors of the two disks can be described by two coupled LLG equations. In the weakly nonlinear regime, those can be effectively approximated in terms of the complex SW amplitudes,

$$c_n = \frac{M_{xn} + iM_{yn}}{\sqrt{M_{sn}(M_{sn} + M_{zn})}}, \quad (3)$$

of disk $n = 1, 2$ [25,43]. At this level of description, the system dynamics can thus be modeled by the stochastic equations

$$\dot{c}_1 = (i - \beta_1)(\omega_1 c_1 + 2p_1 c_1 - h_{12} c_2) + \sqrt{D_1} \xi_1, \quad (4)$$

$$\dot{c}_2 = (i - \beta_2)(\omega_2 c_2 + 2p_2 c_2 - h_{21} c_1) + \sqrt{D_2} \xi_2. \quad (5)$$

These are the equations of motion of two coupled nonlinear oscillators, whose resonance frequencies $\omega_n(p_n) \propto |\mathbf{H}_{\text{eff}}|$ depend on the SW power $p_n = |c_n|^2$ ($n = 1, 2$). The analytical expressions for ω_n at zero temperature, obtained by diagonalizing Eqs. (4) and (5), are given in Refs. [24] and [25]. The damping rates, which describe energy dissipation towards the environment, are chosen to be $\Gamma_n(p_n) = \beta_n \omega_n(p_n)$ [43]. The parameters β_n here model the effect of STT.

Thermal fluctuations are accounted for by the stochastic terms $\sqrt{D_n} \xi_n$, ξ_n being a complex Gaussian random variable with unit variance and zero average, and $D_n = 2\alpha k_B T_n$, as prescribed by the fluctuation-dissipation theorem [43]. This is equivalent to adding a fluctuating term to the effective field in Eq. (1).

The coupling term $h_{12} c_2$ [25] is the functional derivative $i\delta \mathcal{H}_{\text{int}} / \delta c_n^*$ of the interaction Hamiltonian $\mathcal{H}_{\text{int}} = h_{12} c_1 c_2^* + \text{c.c.}$ Note that this Hamiltonian has a general form that describes also exchange interaction, magnon tunneling

between different materials, and phase locking in STNO arrays [37,43].

The chosen form of the stochastic and dissipative terms ensures that, for $\beta_n = \alpha$ and $T_1 = T_2 = T$, the expected canonical distribution $\exp\{-\mathcal{H}/(k_B T)\}$ is the stationary solution of the Fokker-Planck equation associated with Eqs. (4) and (5) (here \mathcal{H} is the Hamiltonian for the isolated system [44]). In this first part of the paper we focus on the case in which $\beta_n = \alpha$. The case when $\beta_n \neq \alpha$, where the system is kept out of equilibrium by STT [45], is also of interest and is discussed in Sec IV.

It is important to remark that Eqs. (4) and (5) hold if the system is dominated by two SW modes, one for each oscillator. In the presence of a texture of the magnetization, the system contains several SW modes, which depend essentially on the geometry of the system [24,25]. This feature can be described by developing Eqs. (4) and (5) in the proper SW mode basis, as in Refs. [24] and [25]. In these systems, thermal fluctuations excite all the SW modes of the system and the intrinsic nonlinearity of the LLG equation generates an additional coupling between the SW modes. The latter can originate complex phenomena, such as mode hopping and mode coexistence [46,47]. In many situations, when the dwelling time between different modes is large enough, one can still use Eqs. (4) and (5) [46]. In our case, it is possible to identify clearly the modes that belong to each oscillator, and the micromagnetic simulations reported in Sec. V corroborate the single-mode picture. In perpendicularly magnetized spin-valve nanopillars with several SW modes, it has been shown that [11,24,25] a SW mode expansion of Eqs. (4) and (5) is sufficient to describe the system properly even in the presence of thermal fluctuations. In particular, no mode hopping as been observed, even in the presence of a thermal gradient [11].

Let us now introduce the conserved currents of the system. Combining Eqs. (4) and (5) with their complex conjugates gives the two conservation equations for the SW power [43],

$$\dot{p}_1 = -2\Gamma_1(p_1)p_1 + j_M^{12}, \quad (6)$$

$$\dot{p}_2 = -2\Gamma_2(p_2)p_2 + j_M^{21}, \quad (7)$$

which leads to the definition of the magnetization current between the two oscillators [44,48]:

$$j_M^{12} = 2h_{12}\text{Im}(c_1c_2^*). \quad (8)$$

Note that Eqs. (6) and (7) are the conservation equations for the z component of the magnetization. For a continuum ferromagnet with exchange stiffness A , they lead to the usual definition of SW spin current $\vec{j}_M = A\vec{M} \times \vec{\nabla}M$ carried by the exchange interaction [21]. The conservation equation for the local energy gives the energy current

$$j_E^{12} = 2h_{12}\text{Re}(\dot{c}_1c_2^*), \quad (9)$$

which describes the transfer of energy between the oscillators. The computation of these currents is similar to the case of the discrete nonlinear Schroedinger equation (see Refs. [44] and [48] for a thorough discussion).

III. PHASE DYNAMICS AND RECTIFICATION

Let us now discuss the rectification effect. A full analytical solution is obtained, in principle, by solving the Fokker-Planck equation associated with Eqs. (4) and (5), in a manner similar to that used in Ref. [49]. For our purposes, it suffices first to restrict ourselves to a discussion of the deterministic equations, obtained by sample averaging Eqs. (4) and (5). Setting $c_n = \sqrt{p_n}e^{i\theta_n}$ and $\phi = \theta_1 - \theta_2$, these equations are written in the phase-amplitude representation as

$$\dot{p}_1 = -2\Gamma_1(p_1)p_1 - j_M^{12} + 2D_1, \quad (10)$$

$$\dot{p}_2 = -2\Gamma_2(p_2)p_2 + j_M^{21} + 2D_2, \quad (11)$$

$$\dot{\phi} = \omega_1(p_1) - \omega_2(p_2) + (h_{21}\sqrt{p_1/p_2} - h_{12}\sqrt{p_2/p_1})\cos\phi, \quad (12)$$

where the currents read $j_M^{12} = 2h_{12}\sqrt{p_1p_2}\sin\phi$ and $j_E^{12} = 2h_{12}\omega_1(p_1)\sqrt{p_1p_2}\sin\phi$. The constant terms $2D_n$ account for the fact that the powers are always bounded away from 0 due to fluctuations. In the context of phase-synchronization phenomena, Eq. (12) is often referred to as the Adler equation [15,17].

The solutions of Eqs. (10)–(12) are of two types: (i) phase-running (desynchronized) solutions, where the two oscillators have different frequencies; and (ii) phase-locked (synchronized) ones. In case i the time-averaged currents are 0, and Eqs. (10)–(12) reduce to $\Gamma_n(p_n) = D_n$ and $\dot{\phi} = \omega_1(p_1) - \omega_2(p_2)$, which implies the equipartition relation $p_n = k_B T_n / \omega_n(p_n)$, for $n = 1, 2$. This means that the thermostats thermalize each oscillator independently and there is *no net transfer* of energy and magnetization between the oscillators. Note that the mere fact that $p_1 \neq p_2$ *does not* imply that there is a net current: the average energy provided by the baths is returned to them. For case ii there is instead a common frequency of oscillation $\dot{\theta}_n = \omega$, so that $\dot{\phi} = 0$ and one has

$$\Gamma_1(p_1) = D_1 - j_M^{12}/2, \quad (13)$$

$$\Gamma_2(p_2) = D_2 + j_M^{21}/2, \quad (14)$$

$$\omega_1(p_1) - \omega_2(p_2) + (h_{21}\sqrt{p_1/p_2} - h_{12}\sqrt{p_2/p_1})\cos\phi = 0. \quad (15)$$

Such a phase-locked regime can only occur if Eqs. (13)–(15) admit a solution, namely, for

$$|\omega_1(p_1) - \omega_2(p_2)| \leq |h_{21}\sqrt{p_1/p_2} - h_{12}\sqrt{p_2/p_1}|. \quad (16)$$

It has to be remarked that, already at this level of approximation, all the parameters are temperature dependent since the spin powers p_1 and p_2 , solutions of Eqs. (13)–(15), depend on both T_1 and T_2 .

The crucial observation is that Eqs. (13) and (14) are not invariant with respect to the exchange of the two noise sources D_1 and D_2 , so there may be regions of the parameters $[D_n, \Gamma_n(p_n)]$ where the currents are different upon exchanging the sign of the applied temperature gradient. In particular, there may be cases in which Eq. (16) is satisfied for, say, $T_1 > T_2$ but

not for $T_1 < T_2$, thus yielding the desired effect. Note also that Eq. (16) defines the condition for the approximate resonance of the effective (temperature-dependent) frequencies and is thus conceptually similar to the criteria of spectral overlap usually invoked to explain the working principle of phononic thermal diodes [8,9].

In the previous analysis, thermal noises are accounted for only through their mean values. In the presence of noise it is known that the phase locking is only effective as fluctuations will eventually desynchronize the oscillators [15,16]. In other words, even when condition (16) holds the phases will not remain exactly locked but will undergo random phase slips leading to phase diffusion.

To substantiate the above arguments, we turn now to numerical simulations of Eqs. (4) and (5). For simplicity, we have taken a symmetric coupling, $h_{12} = h_{21} = h$. At equilibrium, we have set $T_1 = T_2 = T_0$, and then we have increased one of the two temperatures at a time, keeping the other fixed at T_0 and defining the temperature difference as $\Delta T = T_1 - T_2$. After the system has reached a stationary state, the currents were time-averaged over an interval of 10^6 time steps.

Figure 2 shows the two currents vs ΔT , for $\beta_n = \alpha = 0.02$ and $h = 0.1$, averaged over 50 samples. The system clearly displays a rectification effect when $\Delta T > 0$. The two currents have a similar profile, growing monotonically until they reach a plateau at $\Delta T \approx 1.2$. Note that the strength of the rectification effect decreases as T_0 increases.

The origin of the rectification is illustrated in Fig. 3, which shows the power spectra averaged over 500 trajectories. All the following simulations were performed with $T_0 = 0.2$. For positive gradients, the peak at ω_1 broadens and shifts towards a higher frequency, until it overlaps with the peak at ω_2 , while for negative gradients the peaks do not overlap.

When the oscillators are phase locked, the time-averaged currents are not 0 and there is a *net transport* of energy and magnetization through the system. The phase locking

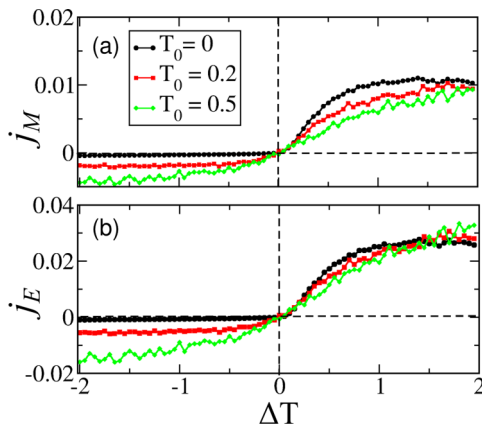


FIG. 2. (Color online) Rectification effect for the magnetization (a) and energy (b) currents, computed for different values of T_0 . Equations (4) and (5) were integrated numerically using a fourth-order Runge-Kutta method with time step 10^{-3} model units, frequencies $\omega_1 = 1$ and $\omega_2 = 2$, and $k_B = 1$.

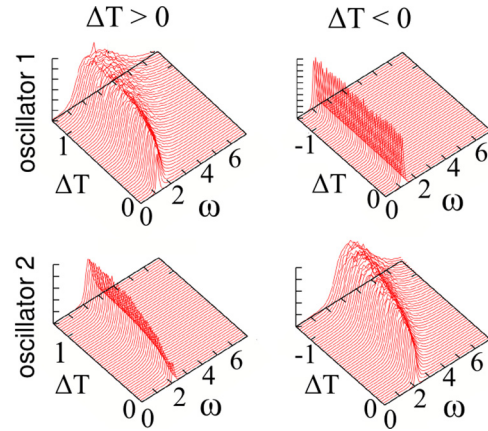


FIG. 3. (Color online) Power spectra of the two oscillators illustrating the mechanism of resonance underlying the rectification effect.

can be seen in Fig. 4(a), which shows the phase difference $\phi = \theta_1 - \theta_2$ vs time, computed for different values of ΔT and averaged over 150 samples. One can see that ϕ is constant in the synchronized regime. The slope $d\phi/dt$, displayed in Fig. 4(b), increases linearly with ΔT and intercepts 0 at $\Delta T = 1.2$, where the oscillators are synchronized and the currents reach the plateau shown in Fig. 2.

We have also investigated the dependence of the current on the damping α and coupling h . Figures 5 and 6 show the phase diagrams of the currents in the planes $(\alpha, \Delta T)$ and $(h, \Delta T)$, respectively. Interestingly, the rectification effect is present in a wide range of system parameters. In both cases, the currents increase with the parameters α and h and vanish around $\alpha \approx 10^{-3}$ and $h \approx 5 \times 10^{-2}$. This feature depends on the fact that α and h control, respectively, the coupling with the thermal baths and between the oscillators.

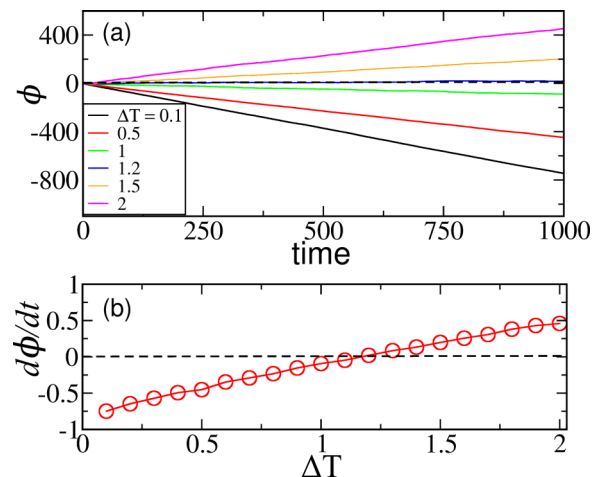


FIG. 4. (Color online) (a) Phase difference ϕ vs time, computed for different values of ΔT . ϕ increases linearly in time in the desynchronized regime, while it is constant in the synchronized one. (b) Slope of ϕ vs ΔT , which vanishes when the oscillators are synchronized. The line is a guide for the eye.

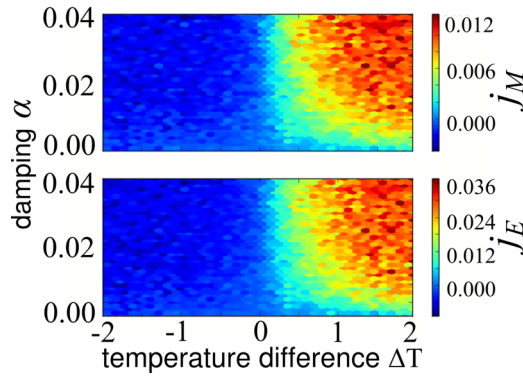


FIG. 5. (Color online) Magnetization and energy currents as a function of the temperature difference ΔT and Gilbert damping parameter α . The currents vanish when the coupling with the bath $\alpha \rightarrow 0$. Data were obtained by averaging the currents over 2×10^6 time steps, with only one trajectory.

IV. COUPLED TRANSPORT

Up to now we have considered the case in which the damping coefficients β_n are set to be equal to the Gilbert damping parameter α . Actually, in STNOs, the damping can be modified by a spin-polarized current [25,37,43], an effect that can be modeled by changing the parameter β_n . This simple fact immediately suggests another route to drive the system off equilibrium. It should in fact be realized that setting $\beta_1 \neq \beta_2$ is somehow equivalent to applying an external force capable of driving energy and magnetization flows. The situation is analogous to the standard nonequilibrium thermodynamics, where the two coupled currents are associated with two “forces”: the differences of temperature and of chemical potential. In our system, the parameters β_n control the escape rate of magnons towards the reservoirs [25,43] and $\Delta\beta = \beta_2 - \beta_1$ acts as an additional force that controls the currents, in a way similar to a chemical potential [44,48].

Taking $h = 0.1$ and $\alpha = 0.02$, the dynamics was computed for different values of ΔT and of the “chemical potential” difference $\Delta\beta$. Computations were performed starting at equilibrium with $\beta_n = \beta_0 = 0.03$ and decreasing one damping while keeping the other fixed at β_0 .

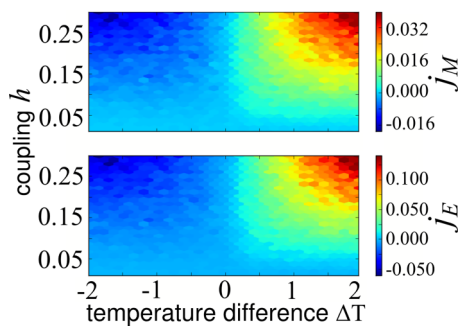


FIG. 6. (Color online) Magnetization and energy currents as a function of the temperature difference ΔT and coupling strength h . The currents vanish when $h \rightarrow 0$, and the oscillators become uncoupled. Data were obtained by averaging the currents over 2×10^6 time steps, with only one trajectory.

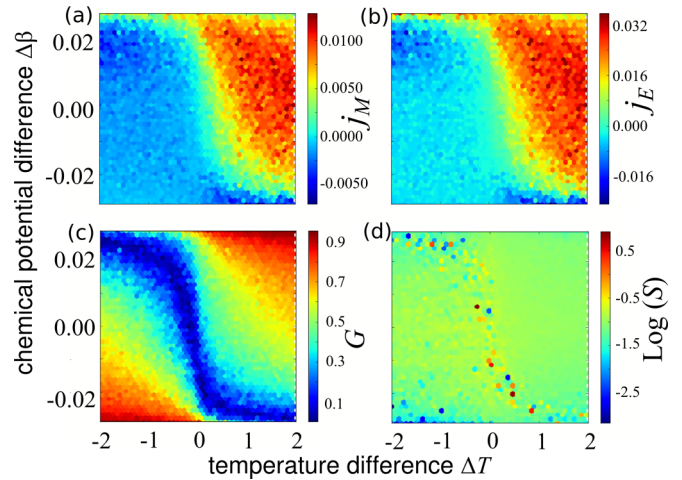


FIG. 7. (Color online) Phase diagrams in the $(\Delta T, \Delta\beta)$ plane. (a) Magnetization and (b) energy currents. (c) Ratio between the spin-wave powers and (d) ratio between the magnetization and the energy currents.

The phase diagrams of the currents are displayed in Figs. 7(a) and 7(b). Both diagrams have a similar profile and are neatly separated into a conducting (yellow-red) and an insulating (light-blue) region. The first occurs at $\Delta T, \Delta\beta > 0$, where oscillator 1 has a lower damping and higher temperature than oscillator 2. When $\Delta T, \Delta\beta < 0$, the situation is reversed and the system is insulating.

One can see here a remarkable feature: When $\Delta\beta$ is sufficiently negative (≈ -0.02), a *negative* current flows at positive ΔT . This means that, with tuning of the chemical potential, the system operates as a *cooling machine* that pumps energy and spin from the colder to the hotter system.

Figure 7(d) shows the power ratio $G = |p_1 - p_2| / (p_1 + p_2)$, which is roughly *symmetric* in the $(\Delta T, \Delta\beta)$ plane. This means that, in both the conducting and the insulating region, there is a similar difference in SW power. In the conducting region, the two oscillators are synchronized and there is a net energy and magnetization transfer from the “hot” to the “cold” system. On the contrary, in the insulating region, there is no current and the energy provided by the baths is returned to them. This corresponds precisely to the situation described at the beginning of the paper: the condition $p_1 \neq p_2$ is *necessary*, but not *sufficient*, to have transport.

An important parameter in spin caloritronics is the spin-Seebeck coefficient, which describes the capability of the system to convert the energy current into a spin current. However, this makes sense only in the linear regime, where the currents are proportional to the thermodynamic forces. Here, the performances of the system can be described by the current ratio $S = |j_M / j_E|$, which is displayed in Fig. 7(d) on a logarithmic scale. In the conducting region, one can see that S is higher in the quasilinear regime (at small ΔT and high $\Delta\beta$), where it reaches 60%, while it decreases smoothly until about 40%–30% as ΔT increases. The current ratio drops to 13% in the inversion regions, where the current becomes negative (positive) with a positive (negative) gradient.

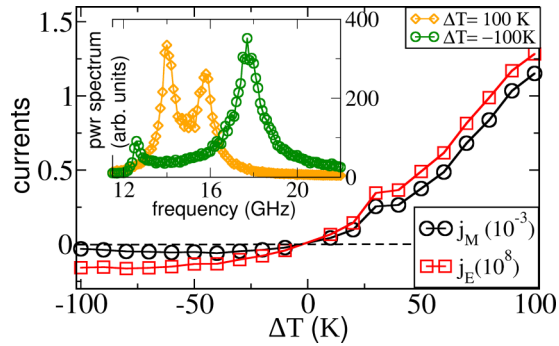


FIG. 8. (Color online) Time-averaged currents vs temperature difference in a spin-valve nano-pillar. Inset: Overlap of the spin-wave modes, at the core of the rectification effect.

V. COMPARISON WITH MICROMAGNETIC SIMULATIONS

To check our model on a realistic system, we have performed micromagnetic simulations on a nanopillar made of two Permalloy (Py) nanodisks, displayed in Fig. 1(a). The disks have a radius $R = 20$ nm, and thicknesses $t_1 = 5$ and $t_2 = 3$ nm, and are separated by a 4-nm spacer. An external field $H_{\text{ext}} = 1$ T is applied along the z direction. The other micromagnetic parameters of the system are as follows. The exchange stiffness of Py is $A = 1.3 \times 10^{-11}$ J/m. The magnetic parameters of the disks, taken from Ref. [24], are $M_{s1} = 7.8 \times 10^5$ A/m, $M_{s2} = 9.4 \times 10^5$ A/m, $\alpha_1 = 1.6 \times 10^{-2}$, $\alpha_2 = 0.85 \times 10^{-2}$, and $\gamma_0 = 1.87 \times 10^{11}$ rad \times s $^{-1}$ \times T $^{-1}$. These parameters are the same as in Refs. [11] and [24]. Computations were performed with the Nmag micromagnetic solver [50], using a finite-element tetrahedral mesh with a maximum size of 3 nm.

Starting from a uniform tilt of the magnetization of 8° with respect to the z direction, the time evolution was computed for 50 ns with a time step of 1 ps, and the results were averaged over 16 samples with different realizations of the stochastic noise.

The time-averaged currents are shown in Fig. 8 as a function of the temperature difference between the two disks. Note that the currents displayed here are per unit coupling and are, thus, pure numbers.

One can see that the system displays a strong rectification effect (compare Fig. 8 with Fig. 2). Moreover, the SW spectra in conducting and insulating regimes are drastically different. Indeed, for negative ΔT the SW spectra display two distinct

maxima, while for positive ΔT there is a single broadened peak (see the inset in Fig. 8). This picture is compatible with the simple double-oscillator model and suggests that the synchronization mechanism proposed above is indeed at the basis of the rectification observed in realistic simulations of the nanopillar.

VI. CONCLUSIONS

To conclude, we have studied, through simple analytical arguments and computer simulations, a novel system which can rectify both energy and magnetization currents. A significant rectification effect is present in a large set of system parameters and the underlying physical process suggests a new method for phase locking and transfer of energy and magnetization in magnonic and spin-caloritronic devices. The connection with phase synchronization phenomena is insightful and allows us to understand the basic rectification mechanism in a simple way.

We wish to stress that the results presented here are general and may apply to systems described by the LLG equation [26–28], with different geometries, coupling mechanisms, and sizes between the nanometer and the micrometer range. The nonlinearity of the LLG equation and the presence of noise are the essential ingredients for this effect. Choosing a spin-valve geometry allows us to study a realistic system where spin transfer also plays a significant role, controlling the magnon population of the device. However, we expect that devices with different geometries (such as nanocontacts of different materials where the spins are exchange coupled) can exhibit a similar rectification effect. At variance with the models studied in the context of phononics [13], the magnonic device allows us to consider coupled transport of the two basic conserved quantities, energy and magnetization. The control of the associated forces allows for new possibilities. As exemplified in this work, it would be possible, for instance, to control the energy current on the device scale by changing the applied spin-polarized currents.

ACKNOWLEDGMENTS

We gratefully acknowledge the Swedish Research Council (V.R.), Carl Tryggers Foundation, and Göran Gustafssons Foundation for financial support. The computer simulations were performed on resources provided by the Swedish National Infrastructure for Computing (SNIC) at the National Supercomputer Centre (NSC).

[1] K. Uchida *et al.*, *Nature* **455**, 778 (2008).
 [2] J. Sinova, *Nat. Mater.* **9**, 880 (2010).
 [3] G. E. U. Bauer, E. Saitoh, and B. J. van Wees, *Nat. Mater.* **11**, 391 (2012).
 [4] S. Lepri, R. Livi, and A. Politi, *Phys. Rep.* **377**, 1 (2003).
 [5] A. Dhar, *Adv. Phys.* **57**, 457 (2008).
 [6] C. W. Chang, D. Okawa, H. Garcia, A. Majumdar, and A. Zettl, *Phys. Rev. Lett.* **101**, 075903 (2008).

[7] A. A. Balandin and D. L. Nika, *Mater. Today* **15**, 266 (2012).
 [8] M. Terraneo, M. Peyrard, and G. Casati, *Phys. Rev. Lett.* **88**, 094302 (2002).
 [9] B. Li, L. Wang, and G. Casati, *Phys. Rev. Lett.* **93**, 184301 (2004).
 [10] K. Saito, G. Benenti, and G. Casati, *Chem. Phys.* **375**, 508 (2010).
 [11] S. Borlenghi, W. Wang, H. Fangohr, L. Bergqvist, and A. Delin, *Phys. Rev. Lett.* **112**, 047203 (2014).

- [12] C. W. Chang, D. Okawa, H. Garcia, A. Majumdar, and A. Zettl, *Phys. Rev. Lett.* **99**, 045901 (2007).
- [13] N. Li, J. Ren, L. Wang, G. Zhang, P. Hänggi, and B. Li, *Rev. Mod. Phys.* **84**, 1045 (2012).
- [14] J. Ren and J.-X. Zhu, *Phys. Rev. B* **88**, 094427 (2013).
- [15] R. L. Stratonovich, *Topics in the Theory of Random Noise, Vol II* (Gordon and Breach, New York, 1967).
- [16] A. Neiman, A. Silchenko, V. Anishchenko, and L. Schimansky-Geier, *Phys. Rev. E* **58**, 7118 (1998).
- [17] A. Neiman, L. Schimansky-Geier, A. Cornell-Bell, and F. Moss, *Phys. Rev. Lett.* **83**, 4896 (1999).
- [18] J. Teramae and D. Tanaka, *Phys. Rev. Lett.* **93**, 204103 (2004).
- [19] W. Singer, *Neuron* **24**, 49 (1999).
- [20] S. Bahar, A. Neiman, L. A. Wilkens, and F. Moss, *Phys. Rev. E* **65**, 050901 (2002).
- [21] S.-K. Kim, *J. Phys. D* **43**, 264004 (2010).
- [22] V. V. Kruglyak, S. O. Demokritov, and D. Grundler, *J. Phys. D* **43**, 264001 (2010).
- [23] A. Khitun, M. Bao, and K. L. Wang, *J. Phys. D* **43**, 264005 (2010).
- [24] S. Borlenghi, Ph.D. thesis; available at: <http://tel.archives-ouvertes.fr/tel-00590363/>
- [25] V. V. Naletov *et al.*, *Phys. Rev. B* **84**, 224423 (2011).
- [26] L. D. Landau and E. M. Lifshitz, in *Collected Papers* (Pergamon Press, Oxford, UK, 1965).
- [27] T. Gilbert, *IEEE, Trans. Magnet.* **40**, 3443 (2004).
- [28] A. G. Gurevich and G. A. Melkov, *Magnetization Oscillation and Waves* (CRC Press, Boca Raton, FL, 1996).
- [29] J. Slonczewski, *J. Magn. Magn. Mater.* **159**, L1 (1996).
- [30] L. Berger, *Phys. Rev. B* **54**, 9353 (1996).
- [31] H. Kubota, A. Fukushima, K. Yakushiji, T. Nagahama, S. Yuasa, K. Ando, H. Maehara, Y. Nagamine, K. Tsunekawa, D. D. Djayaprawira, N. Watanabe, and Y. Suzuki, *Nat. Phys.* **4**, 37 (2007).
- [32] J. C. Sankey, Y.-T. Cui, J. Z. Sun, J. C. Slonczewski, R. A. Buhrman, and D. C. Ralph, *Nat. Phys.* **4**, 67 (2008).
- [33] S. Petit, N. de Mestier, C. Baraduc, C. Thirion, Y. Liu, M. Li, P. Wang, and B. Dieny, *Phys. Rev. B* **78**, 184420 (2008).
- [34] M. H. Jung, S. Park, C.-Y. You, and S. Yuasa, *Phys. Rev. B* **81**, 134419 (2010).
- [35] X. Jia, K. Xia, Y. Ke, and H. Guo, *Phys. Rev. B* **84**, 014401 (2011).
- [36] J. A. Katine, F. J. Albert, R. A. Buhrman, E. B. Myers, and D. C. Ralph, *Phys. Rev. Lett.* **84**, 3149 (2000).
- [37] J. A. Katine and E. E. Fullerton, *J. Magn. Magn. Mater.* **320**, 1217 (2008).
- [38] A. Brataas, G. E. Bauer, and P. J. Kelly, *Phys. Rep.* **427**, 157 (2006).
- [39] A. Brataas, Y. V. Nazarov, and G. E. W. Bauer, *Phys. Rev. Lett.* **84**, 2481 (2000).
- [40] X. Waintal, E. B. Myers, P. W. Brouwer, and D. C. Ralph, *Phys. Rev. B* **62**, 12317 (2000).
- [41] V. S. Rychkov, S. Borlenghi, H. Jaffres, A. Fert, and X. Waintal, *Phys. Rev. Lett.* **103**, 066602 (2009).
- [42] S. Borlenghi, V. Rychkov, C. Petitjean, and X. Waintal, *Phys. Rev. B* **84**, 035412 (2011).
- [43] A. Slavin and V. Tiberkevich, *IEEE Trans. Magn.* **45**, 1875 (2009).
- [44] S. Iubini, S. Lepri, R. Livi, and A. Politi, *J. Stat Mech.* (2013) P08017.
- [45] V. Tiberkevich, A. Slavin, and J.-V. Kim, *IEEE Trans. Magn.* **91**, 192506 (2007).
- [46] P. K. Muduli, O. G. Heinonen, and J. Akerman, *Phys. Rev. Lett.* **108**, 207203 (2012).
- [47] O. Heinonen, Y. Zhou, and D. Li, [arXiv:1310.6791v2](https://arxiv.org/abs/1310.6791v2).
- [48] S. Iubini, S. Lepri, and A. Politi, *Phys. Rev. E* **86**, 011108 (2012).
- [49] S. Liu, B. K. Agarwalla, J.-S. Wang, and B. Li, *Phys. Rev. E* **87**, 022122 (2013).
- [50] T. Fischbacher *et al.*, *IEEE Trans. Magn.* **43**, 2896 (2007).